Pharmaceutical Research, Vol. 25, No. 10, October 2008 (© 2008)
DOI: 10.1007/s11095-008-9619-y

Research Paper

Designing 3D Photopolymer Hydrogels to Regulate Biomechanical Cues and Tissue Growth for Cartilage Tissue Engineering

Stephanie J. Bryant,[1,2] Garret D. Nicodemus,[1] and Idalis Villanueva[1]

Received February 23, 2008; accepted April 29, 2008; published online May 29, 2008

Purpose. Synthetic hydrogels fabricated from photopolymerization are attractive for tissue engineering for their controlled macroscopic properties, the ability to incorporate biological functionalities, and cell encapsulation. The goal of the present study was to exploit the attractive features of synthetic hydrogels to elucidate the role of gel structure and chemistry in regulating biomechanical cues.
Methods. Cartilage cells were encapsulated in poly(ethylene glycol) (PEG) hydrogels with different crosslinking densities. Cellular deformation was examined as a function of gel crosslinking. The effects of continuous *versus* intermittent dynamic loading regimens were examined. RGD, a cell adhesion peptide, was incorporated into PEG gels and subjected to mechanical loading. Chondrocyte morphology and activity was assessed by anabolic and catabolic ECM gene expression and matrix production by collagen and glycosaminoglycan production.
Results. Cell deformation was mediated by gel crosslinking. In the absence of loading, anabolic activity was moderately upregulated while catabolic activity was significantly inhibited regardless of gel crosslinking. Dynamic loading enhanced anabolic activities, but continuous loading inhibited catabolic activity, while intermittent loading stimulated catabolic activity. RGD acted as a mechanoreceptor to influence tissue deposition.
Conclusions. We demonstrate the ability to regulate biomechanical cues through manipulations in the gel structure and chemistry and cartilage tissue engineering.

KEY WORDS: cartilage; hydrogel; photopolymerization; tissue engineering.

INTRODUCTION

Tissue engineering is a promising approach for replacing damaged and/or diseased tissues with healthy living tissues that can ultimately restore long-term tissue and/or organ function. One common approach is to utilize a 3D scaffold that serves as a temporary support for cell growth and new tissue development.

Photopolymerized hydrogels are particularly attractive as tissue engineering scaffolds for several reasons. Hydrogels, in general, exhibit high water contents, often greater than 80% water, and exhibit tissue-like elastic properties making them ideal candidates for creating environments that promote cell and tissue growth (1). *Photo*polymerization allows for spatial control over the polymerization reaction enabling facile fabrication of complex 3D architectures. The mild reaction conditions, which can be performed at physiological pH and temperature, enable cell and protein encapsulation as well as *in vivo* gelation (2–4). In addition, macroscopic gel properties (e.g., mechanical properties, water contents) and degradation profiles are readily tunable through changes in the degree of crosslinking and the gel chemistry (1,5,6). Lastly, synthetic and natural polymers which exhibit appropriate functional groups can be modified with photoreactive moieties (e.g., (meth)acrylate) to create 3D environments suitable for a wide range of tissue engineering applications (7–14).

Together, these attributes make photopolymerized hydrogels particularly attractive for tissue engineering. As such, photopolymerized hydrogels have been used as cell carriers for a number of tissue engineering applications including cartilage (14–18), bone (19–21), nerve (22), liver (23), and more recently for maintaining undifferentiated human embryonic stem cells in long term 3D cultures (24). Our research group is particularly interested in exploiting the gel architecture and chemistry of photopolymerized hydrogels to promote functional tissue growth for cartilage tissue engineering.

One of the attractive features of synthetic hydrogels is the ability to control the macroscopic properties of the gel through simple changes in gel crosslinking. For example, the crosslinking density influences many properties important in the design of a tissue engineering scaffold including the compressive modulus, water content, and diffusion (25–27). In designing an *in situ* forming hydrogel cell carrier for tissues where mechanical forces are prevalent, the gel structure will also play a key role in translating the applied mechanical forces into biomechanical cues (e.g., through cell deformation and mechanoreceptors). Because cells and proteins do not interact with poly(ethylene glycol) (PEG), it serves as an

[1] Department of Chemical and Biological Engineering, University of Colorado, Boulder, Colorado 80309-0424, USA.
[2] To whom correspondence should be addressed. (e-mail: sbryant@colorado.edu)

excellent base from which to explore the role of cell deformation on cell function. Matrix analogs can then be systematically incorporated into the PEG gels to introduce cell-matrix interactions to study the role of mechanoreceptors in a highly controlled environment. In this study, we examine the roles of (1) gel structure in controlling cell deformation and chondrocyte activity; (2) two dynamic loading regimes (continuous *versus* intermittent) in controlling chondrocyte activity; and (3) RGD, a well-known cell adhesion moiety, as a mechanoreceptor in controlling chondrocyte activity. Chondrocyte activity was assessed by gene expression for anabolic and catabolic extracellular matrix molecules or newly synthesized tissue deposition. Together, this information will aid in designing hydrogels to regulate biomechanical cues to facilitate optimal cartilage growth.

MATERIALS AND METHODS

Hydrogel Formation

Poly(ethylene glycol) (PEG, 3,000 Da, Fluka) was reacted with methacryloyl chloride (Sigma) or acryloyl chloride (Sigma) in the presence of triethylamine (Sigma) for 24 h at 4°C. The final PEG macromer product, poly (ethylene glycol) dimethacrylate (PEGDM) or polyethylene glycol diacrylate (PEGDA), was purified by precipitations in ethyl ether and analyzed using ^{1}H NMR (Varian YVR-500S). The degree of substitution was greater than 80%. To create cylindrical gels (5×5 mm), PEGDM was dissolved in phosphate buffered saline (PBS, pH 7.4, Invitrogen) at 10%, 20% or 30% (*w*/*w*) and mixed with 0.05%, 0.0125%, or 0.0056% (*w*/*w*) photoinitiator (Irgacure I2959, Ciba Specialty Chemical), respectively, and exposed to 365 nm light (UVP, Model XX-20) at 6 mW/cm^2 for 10 min to form low, medium and high crosslinked gels, respectively.

To study the role of cell–matrix interactions in the form of mechanoreceptors, the cell adhesion ligand, RGD, was incorporated into the PEG hydrogel network. In brief, a 10% molar excess of NH_2-Tyr-Arg-Gly-Asp-Ser-COOH (YRGDS, Bachem) (1 mg/ml) was reacted with acryloyl-PEG-*N*-hydroxysuccinimide (ACR-PEG-NHS) (3,400 Da, Nektar) (10 mg/ml) in 50 mM of bicarbonate buffer (pH=8.4) for 2 h. A fluoraldehyde assay (Pierce) was used to assess indirectly the efficiency of the reaction by measuring the amount of unreacted primary amines, which was determined to be greater than 85%. The final product, ACR-PEG-RGD was dialyzed overnight and lyophilized for 24 h. ACR-PEG-RGD (0, 0.1, 0.4, and 0.8 mM) was added to 10% *w*/*w* PEGDA with 0.05% *w*/*w* Irgacure 2959 and polymerized as described above.

Cell Isolation and Culture

Chondrocytes were isolated from full depth articular cartilage harvested from the patellar-femoral groove of 1- to 3-week-old calves (Research 87) or from the metacarpalphalangeal joints of front feet from 2- to 4-year-old steers (Arapahoe Packing) within 24 h of slaughter. The former isolation was employed in studies described by Figs. 2 and 3 and the latter isolation was employed for studies described by Figs. 1 and 4. Explanted cartilage was digested in 500 U/ml collagenase II (Worthington Biochemical) in Dulbecco's minimal essential medium (DMEM, Invitrogen) supplemented with 5% fetal bovine serum (FBS, Invitrogen) for 16 h at 37°C. Isolated chondrocytes were washed and resuspended in chondrocyte media (DMEM supplemented with 20% FBS (*v*/*v*), 0.04 mM L-proline (Sigma), 50 mg/l L-ascorbic acid (Sigma), 10 mM HEPES buffer (Invitrogen), 0.1 M MEM-nonessential amino acids (Invitrogen), 1% penicillin–streptomycin (Invitrogen), 0.5 μg/ml fungizone (Invitrogen), and 20 μg/ml gentamicin (Invitrogen)). Chondrocytes at 50 million cells/ml were combined with sterile macromer solution and photopolymerized as described above. Cell-laden hydrogel constructs were allowed to equilibrate under free swelling conditions for 24 h in cell culture media in a humid environment at 37°C and 5% CO_2 prior to loading mechanically.

Cell and Matrix Visualization

To visualize chondrocytes encapsulated into hydrogels, a fluorescent membrane integrity assay, LIVE/DEAD® Assay

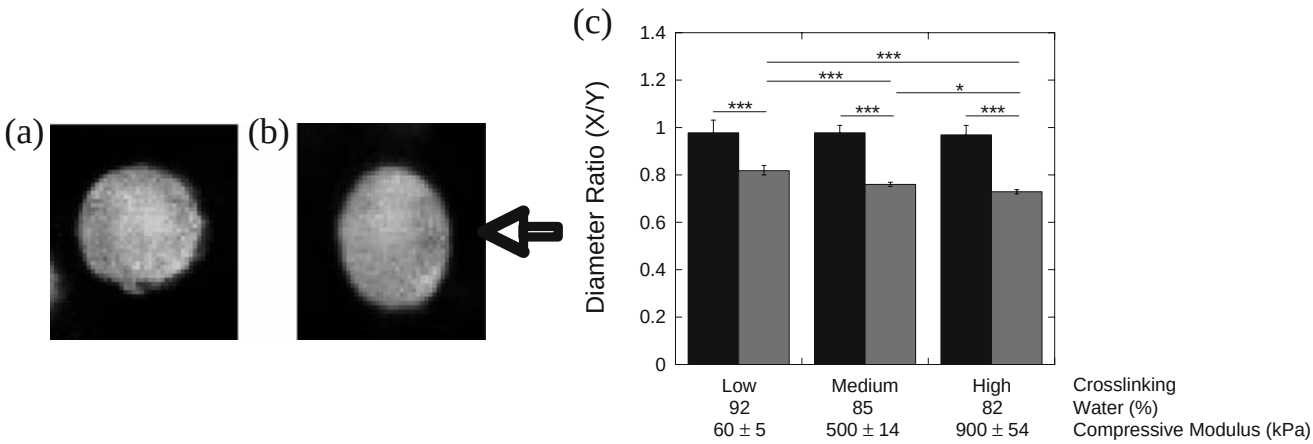

Fig. 1. A live cell encapsulated in a low crosslinked PEG hydrogel subjected to no strain (**a**) and subjected to a 15% strain (**b**). Cell deformation was quantified by diameter ratio as a function of gel crosslinking under no strain (*black bars*) and subjected to an applied 15% strain (*gray bars*). The macroscopic properties (i.e., equilibrium water content (%) and compressive modulus (kPa)) of the gels are also provided as a function of gel crosslinking. (*$p<0.05$; ***$p<0.001$).

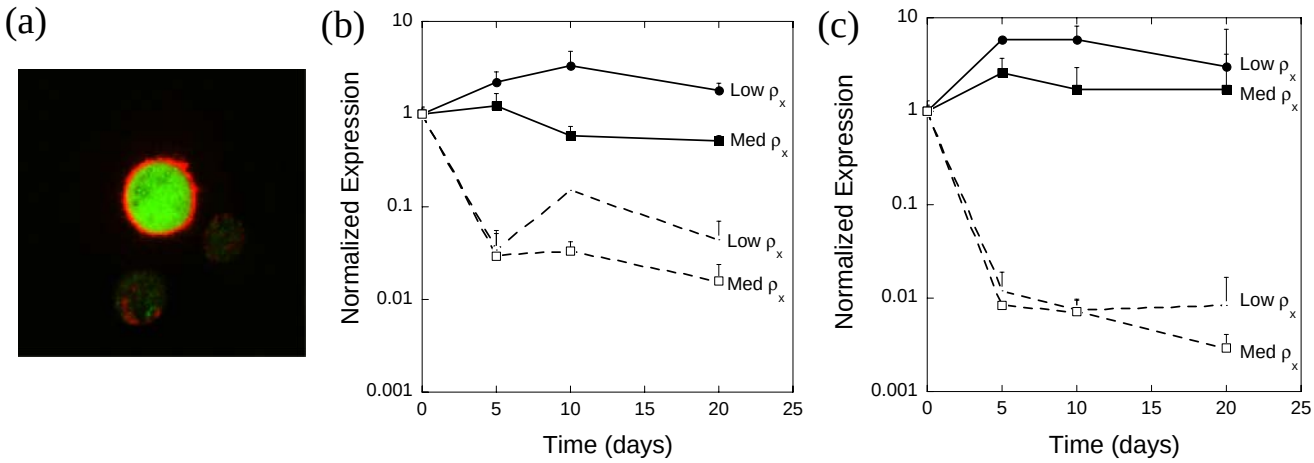

Fig. 2. A live cell (*green*) surrounded by a newly synthesized pericellular matrix (*red*) 3 days post-encapsulation in a low crosslinked PEG hydrogel (**a**). The effects of hydrogel structure in the form of crosslinking density and culture time on anabolic and catabolic gene expression (**b**, **c**). Anabolic gene expression was measured by collagen type II (**b**, *solid line*) and aggrecan (**c**, *solid line*). Catabolic gene expression was measured by MMP-1 (**b**, *dotted line*) and MMP-3 (**c**, *dotted line*). The data were normalized to day 0 expression levels.

(Invitrogen) where live cells fluoresce green and dead cells fluoresce red was employed. Hydrogels were treated with 5 μM calcein-AM and 2 μM ethidium homodimer for 30 min. For matrix visualization *in situ*, an immunofluorescent approach was employed. The hydrogels were placed in PBS supplemented with 0.5 U/ml Chondroitinase ABC (Sigma) and 1% BSA (Sigma) to expose the chondroitin sulfate epitope for 1 h. Hydrogels were treated with anti-chondroitin-6-sulfate (clone MK-302, Chemicon) (1:50) in DMEM+20% FBS for 1 h, rinsed with Earle's Balanced Salt Solution (EBSS, Gibco), and placed in DMEM+20% FBS with goat anti-mouse IgG labeled with Alexa Fluor 546 (1:20) (Invitrogen) for 1 h. Cytoplasm was counterstained with 5 μM calcein-AM for 30 min.

Cell Deformation

Chondrocyte-laden hydrogel constructs were allowed to swell for 72 h prior to placing in a custom designed hydrogel strainer apparatus similar to that described by Knight *et al.* (28). The hydrogel strainer sits on the stage of an inverted microscope associated with a confocal laser scanning unit (Zeiss LSM 510). Hydrogels were subjected to 15% compressive strain. Images were captured at full width half

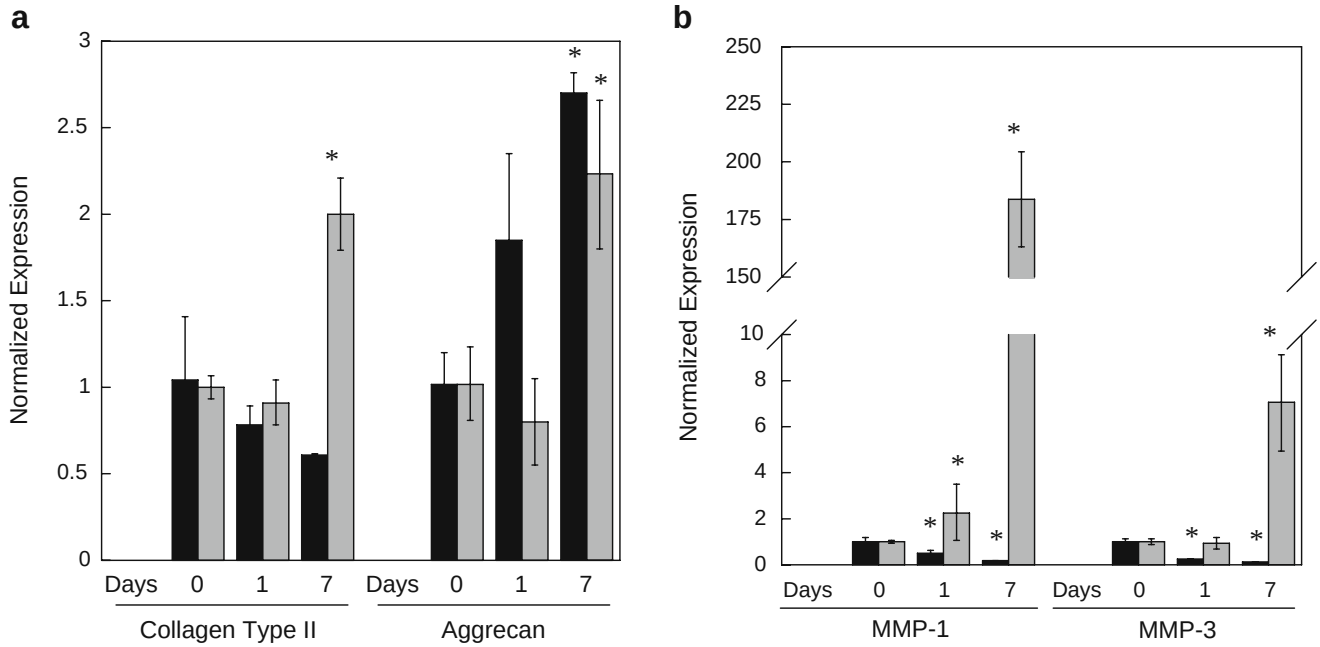

Fig. 3. The effects of dynamic loading regime on chondrocyte anabolic and catabolic activity within a low crosslinked PEG gel. Two loading regimes were examined: continuous dynamic loading at 0.3 Hz and 15% amplitude strains (*black bars*) and intermittent dynamic loading at 0.3 Hz and 15% amplitude strains (12 h off, 1 h on/1 h off for 12 h) (*gray bars*). Gene expression was normalized to day 0 time point (i.e., 24 h post-encapsulation and immediately prior to loading). $^{*}p<0.05$ compared to day 0, $^{\dagger}p<0.05$ compared to continuous loading. **a** represents anabolic gene expression and **b** represents catabolic gene expression.

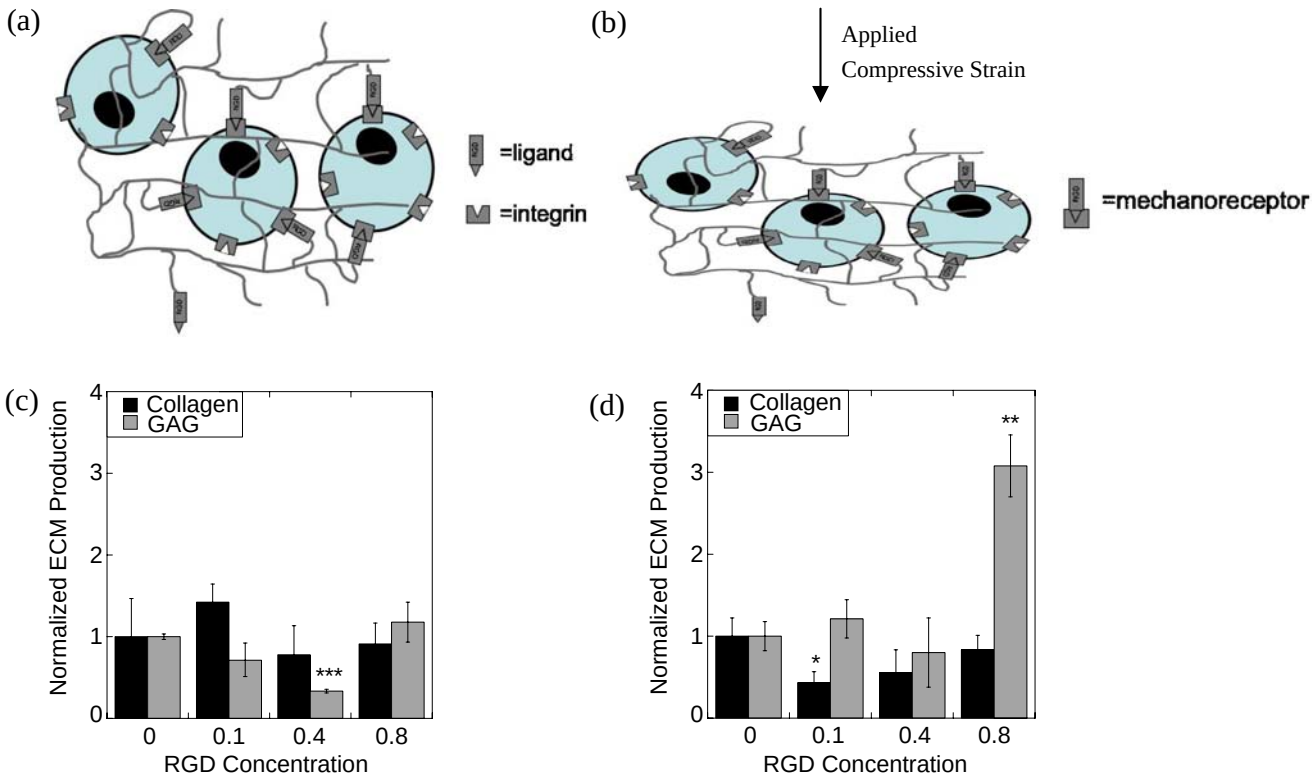

Fig. 4. Schematic of PEG-RGD gels in which the RGD ligand binds to its corresponding integrin on the cell membrane (**a**). When a compressive strain is applied to the PEG-RGD constructs, the RGD ligand-integrin bond may act as a mechanoreceptor to regulate chondrocyte function (**b**). Chondrocyte response was measured by newly synthesized matrix, total collagen production (*black bars*) and glycosaminoglycan production (*gray bars*), in the absence of loading (**c**) and when subjected to dynamic loading (0.3 Hz, 15% amplitude strains) (**d**). The data was normalized to the 0 mM RGD hydrogel. Data is reported as mean±standard deviation. An *asterisk*(*s*) above a bar indicates a significant difference from 0 mM RGD (*$p<0.05$; **$p<0.01$; ***$p<0.001$). In **d**, *asterisk*(*s*) also indicates a significant difference compared to 0.1 and 0.4 mM RGD samples ($p<0.01$).

maximum height immediately after the application of the applied strain. The level of cellular strain remained constant during the experiment (~1 h, unpublished results). A total of 48 cells were imaged from three regions of interest per hydrogel composition (two gels were imaged per formulation, $n=96$). Cell morphology was quantified by a diameter ratio (x/y) where x represents the cell diameter parallel to the applied strain and y represents the cell diameter perpendicular to the applied strain (28,29).

Mechanical Loading

Custom-built loading apparatuses previously described by the authors were employed to apply dynamic compressive strains to the cell-laden hydrogel constructs (30,31). Briefly, each loading apparatus uses a standard 24-well tissue culture plate in which one gel is placed in each well and has a corresponding loading platen. Frequency, strain and duration are readily controlled by an external computer. The low crosslinked gels were employed in the dynamically loaded experiment. Due to the weight of the platen, a 5% offset strain was applied to the hydrogel. Dynamic loading was performed by applying a sinusoidal waveform from 5% to 20% maximum strain with a frequency of 0.3 Hz. For data presented in Fig. 3, the gels were dynamically loaded for 1 and 7 days either continuously or intermittently (12 h off, 1 h on/1 h off for 12 h). For data presented in Fig. 4, the gels were dynamically loaded for 2 days continuously. At specified time points, samples were removed. Chondrocyte media was replaced every 2 days. Free swelling gels were cultured in 24 well culture plates and used as unstrained controls. Cell viability was qualitatively assessed using a LIVE/DEAD® Assay (Invitrogen) and was high under all conditions.

Gene Expression

At specific time points, loaded or unloaded gels were removed and immediately homogenized under liquid nitrogen and subsequently processed with TRI Reagent (Sigma) to isolate total RNA (32). RNA was quantified using Ribogreen RNA Quantification Kit (Invitrogen) or the Nanodrop (ND-1000, Thermo-Fisher). RNA (100 ng to 1 μg) was treated with Turbo DNA-free (Ambion) and transcribed using the High Capacity cDNA Kit (Applied Biosystems). Real-time RT-PCR (ABI 7500Fast) was performed using custom designed and validated D-LUX primers for L30, collagen II, aggrecan, MMP-1, and MMP-3 with the Taqman® Fast Universal PCR Master Mix (Applied Biosystems). Primers for L30, collagen II and aggrecan have been previously reported by the authors (31). For MMP-1, forward primer is cggtcAGAAGT-GATGTTCTTCAAAGAC[c-FAM]G and reverse primer is TCCACTTCTGGGTACAAGGGATTT resulting in an

amplicon length of 68 bp. For MMP-3, forward primer is cgttcCTCCAGCACTCAACCGAA[c-JOE]G and reverse primer is AGGTCTGTGCGAGGGTCGTAG resulting in an amplicon length of 67 bp. Data are presented as:

$$Normalized\ Expression = \frac{E_{(GOI)}^{\Delta C_{T(GOI)}(Calibrator-sample)}}{E_{(HKG)}^{\Delta C_{T(HKG)}(Calibrator-sample)}}$$

where E is the efficiency of the gene amplification, GOI is the gene of interest, HKG is the housekeeping gene (L30), and C_T is the cycle threshold point. The samples were normalized to a calibrator (e.g., day 0 samples). L30, a mitochondrial ribosomal protein, was used as the HKG (33) because it was stable throughout the experiments (unpublished data). A sample size of three was used.

Biochemical Analysis

At specified time points, gels were removed, homogenized and digested in a papain enzymatic solution [125 mg/ml of papain (Worthington Biochemical), 10 mM of L-cysteine–HCl (Sigma), 100 mM of phosphate (Sigma) and 10 mM of ethylenediaminetetraacetic acid (Biorad) at a pH of 6.3 for 16 h at 60°C]. Hydroxyproline was measured as an indication of the total collagen content in the digests (34). Glycosaminoglycan content was measured in the papain digests using the dimethylmethylene blue dye (Sigma) method (35). Hoeschst 33258 fluorescence assay (Polysciences) was used to quantify total DNA content in the papain digest (36). All biochemical data were normalized to total DNA content. A sample size of three was used.

Hydrogel Characterization

Cell-free cylindrical hydrogels (5×5 mm) were swollen for 24 h to equilibrium in PBS at 37°C. To measure the equilibrium water content, the equilibrium swollen mass was measured. The gel was subsequently dried by lyophilization for 24 h and the dry polymer mass measured. The tangent compressive modulus (MTS Synergie 100) was determined by applying a constant strain rate of 0.02 mm/s to the hydrated hydrogels in unconfined compression and the resulting stress recorded. A sample size of five to six was used for gel characterization.

Statistical Analysis

Data are represented as mean±standard deviation. Normalized gene expression values were analyzed using ANOVA and Tukey *post hoc* to determine the statistical significance. A confidence level of 0.95 was considered significant.

RESULTS AND DISCUSSION

The Role of Hydrogel Structure in Regulating Cell Deformation

Cell deformation is thought to be one mechanism by which chondrocytes sense mechanical loads (37,38). To explore the role of gel structure in regulating cell deformation, chondrocytes were encapsulated in PEG hydrogels of three crosslinking densities (i.e., low, medium and high) and cultured under free swelling conditions for 3 days. At day 3, the gels were subjected to a 15% compressive strain and their morphology assessed. A representative image of a chondrocyte encapsulated in the low crosslinked PEG hydrogel and subjected to no strain and a gross 15% compressive strain is shown in Fig. 1a and b, respectively. Cell deformation was quantitatively assessed by a diameter ratio where a value of one indicates a spherical cell and a value less than one indicates the cell has deformed under the applied gross strains. The results are shown in Fig. 1c. In the absence of an applied strain, the diameter ratios were unity for all gel crosslinking densities suggesting the encapsulated cells adopted a round morphology. However, the application of a compressive strain resulted in a significant decrease in the diameter ratio in all three gels. Interestingly, the level of cell deformation was dependent on the degree of crosslinking and was highest in gels with the highest crosslinking density. The hydrogel macroscopic properties were also evaluated (Fig. 1c) in which the water contents were greater than 80% in all gels, while the compressive moduli spanned from 60 to 900 kPa. Our findings suggest that synthetic crosslinked hydrogels offer a mechanism to control the level of cell deformation through changes in the crosslinking density. A recent study by our group described the effects of PEG gel crosslinking on early chondrocyte response when subjected to static or dynamic loading for 48 h. Cell proliferation and proteoglycan synthesis were found to be highly dependent on the degree of crosslinking and the loading regimen suggesting that the degree of cell deformation may, in part, control chondrocyte activity (30).

The Role of Hydrogel Structure in Regulating Chondrocyte Activity

In cartilage homeostasis, chondrocytes are responsible for turnover of new matrix where there is a balance between anabolic and catabolic activities. Elucidating these activities as a function of scaffold and culture environment is important in designing a scaffold to promote new tissue growth. In the absence of an applied load, the hydrogel structure may influence chondrocyte activity due to the crosslinks. Previous studies by Bryant and Anseth (1) demonstrated that the crosslinking density of PEG gels influences the distribution of newly synthesized matrix where gels with high crosslinking restrict diffusion of matrix molecules into the extracellular regions of the gel. Therefore in this study, we initially assessed the role of gel structure in regulating anabolic and catabolic activities under free swelling conditions.

Within several days post-encapsulation chondrocyte anabolic activity involves depositing a pericellular matrix. Fig. 2a illustrates a representative image of a live chondrocyte after being encapsulated in a low crosslinked gel for 3 days. The cell is surrounded by newly synthesized matrix where proteoglycans are stained red. It is likely that the formation of this pericellular matrix is an innate response of the chondrocyte when placed in a new environment (39). To assess anabolic and catabolic chondrocyte activities as a function of gel crosslinking, free swelling hydrogels of two different crosslinking densities were examined. Specifically, we chose

to explore the low and medium crosslinked gels. Gene regulation of two major extracellular matrix (ECM) proteins, collagen II and aggrecan, was assessed for anabolic activity. Gene regulation for catabolic activity was assessed by measuring matrix metalloproteinases (MMP). Specifically, we examined MMP-1, which is responsible for cleaving collagen (including collagen II) and MMP-3, which is responsible for cleaving aggrecan. The results are shown in Fig. 2b for collagen II and MMP-1 expressions and in Fig. 2c for aggrecan and MMP-3 expression.

Gene expression was normalized to day 0 expression and followed over a 20 day culture period. Collagen II expression increased slightly in the low crosslinked gel up to day 10, but by day 20, expression levels were similar to day 0. A decrease in collagen II expression, however, was observed with the medium crosslinked gel with culture time. Aggrecan expression for the low crosslinked gels significantly increased with culture time up to day 10 but by day 20 was statistically similar to day 0. For the medium crosslinked gel, aggrecan expression did not significantly change with culture time, but was statistically lower compared to the low crosslinked gel at days 5 and 10. Overall, catabolic activities were significantly down regulated within 5 days of culture by 10-fold for MMP-1 and 100- to 1,000-fold for MMP-3 regardless of gel crosslinking. These results suggest that free swelling PEG hydrogels support anabolic gene expression, with the highest expression levels seen in the low crosslinked gel, and inhibits catabolic activities.

The Role of Dynamic Loading Regime in Regulating Chondrocyte Activity

Mechanical loading plays an integral role in cartilage homeostasis but the optimal conditions for *in vitro* culture remain elusive and is likely to be dependent on the scaffold architecture and its chemistry. Here, we chose to utilize the low crosslinked gel because of its role in enhanced anabolic activities to explore two loading regimes. Specifically, a continuous and intermittent dynamic loading regime was chosen to understand the importance of loading duration on chondrocyte activity during early culture times of up to 1 week. Dynamic compressive strains were applied for 1 week continuously or intermittently (12 h off, 1 h on/1 h off for 12 h). During each loading cycle the cell will undergo deformation in which cells cultured under the continuous loading regime will experience four times more cycles (and deformations) compared to the intermittent regime. Early chondrocyte response was assessed by measuring anabolic and catabolic gene expression at day 0 (i.e., 24 h post-encapsulation), day 1, and day 7. Gene expression was normalized to day 0 time point and the results are given in Fig. 3.

Gels cultured under continuous dynamic loading conditions led to an up-regulation in anabolic activities (specifically aggrecan) and a down regulation in catabolic activities. By day 7, a threefold increase in aggrecan expression, fivefold decrease in MMP-1 expression, and 10-fold decrease in MMP-3 expression were observed. When gels were subjected to intermittent loading conditions, chondrocytes behaved much differently. By day 7, collagen II and aggrecan expression were up-regulated by approximately twofold; however, MMP-1 and MMP-3 levels increased by approximately 180-fold and sevenfold, respectively.

Our results illustrate that continuous dynamic loading moderately stimulates anabolic activity, but down regulates catabolic activity while intermittent dynamic loading leads to a moderate stimulation of anabolic activity but a significant up-regulation in catabolic activities. Our findings are contrary to our expectations in which others have suggested that intermittent loading is desirable for tissue deposition while continuous loading may be interpreted as overloading and negatively impact tissue growth (40,41). There are several possible explanations. During the *off* period in the intermittent loading regime, the gels are subject to the weight of the loading platen, which for the low crosslinked gels, inherently causes a ~5% strain on the gels. Static strains have been shown to increase MMP activity in cartilage explants (42) and in chondrocyte seeded scaffolds (43,44). However, an integral part of the remodeling process of the ECM is the initial breakdown of matrix following reorganization and synthesis of new matrix. Therefore, stimulation of both anabolic and catabolic activities may be important in improving overall tissue formation (43). Additional studies, however, are needed to understand fully the responses observed here.

The Role of Mechanoreceptors in Regulating Chondrocyte Activity

The ECM of cartilage is comprised predominantly of collagen II and aggrecan. However, chondrocytes are surrounded by a very different matrix called the pericellular matrix (PCM), which is rich in collagen types II, VI, IX, fibronectin and aggrecan (39,45). Cellular interactions with the "information rich" PCM result in "outside-in" signaling mechanisms, which regulate many biological processes such as cell growth, differentiation and overall tissue maintenance (39). Fibronectin, one of the proteins found in the PCM, binds to cell surface receptors through the short oligopeptide sequence, Arg-Gly-Asp (RGD) (46). The RGD sequence has been shown to be essential for chondrocyte adhesion to fibronectin coated surfaces (47) and has been shown to enhance chondrogenesis of human mesenchymal stems when encapsulated in PEG hydrogels (48).

Therefore, this study investigated if RGD can act as a mechanoreceptor and its biomechanical role in regulating chondrocyte function and tissue deposition. Specifically, RGD was tethered to a low crosslinked PEG hydrogel as depicted in Fig. 4a by incorporating varying concentrations of an acryloyl modified RGD (0, 0.1, 0.4 and 0.8 mM). It is important to note that the final concentration of RGD was not assessed in the gels. In addition, the incorporation of RGD did not affect the mechanical properties (i.e. compressive modulus) or the water content of the hydrogels. When subjected to an applied compressive strain, the integrin–ligand interaction may also undergo strain and serve as a mechanical transducer (Fig. 4b). In order to elucidate concentration effects of RGD, we chose to study chondrocyte response at very early culture times of up to 3 days (1 day of free swelling culture and 2 days of loading) to minimize the cell–matrix interaction that result from newly synthesized matrix.

Initially, we explored the role of RGD on matrix production in the absence of mechanical loading. To isolate

the effects of RGD, PEG-RGD gels were normalized to PEG gels which did not contain RGD. Newly synthesized matrix molecules were analyzed by measuring total collagen and glycosaminoglycan contents. Interestingly, the incorporation of RGD into the hydrogels had little effect on matrix production (Fig. 4c). Specifically, there was no affect on collagen production at the RGD concentrations studied. A down regulation in GAG production was observed in the 0.4 mM RGD gels, but reached similar values with 0.8 mM RGD. To study the effects of RGD as a mechanoreceptor, dynamically loaded PEG-RGD gels were normalized to loaded PEG gels which did not contain RGD. Interestingly, the addition of 0.1 mM RGD resulted in a significant inhibition in total collagen production, but this inhibition was fully recovered with higher amounts of RGD. On the contrary, GAG production was not affected by the addition of low amounts of RGD, but 0.8 mM RGD resulted in a threefold increase in GAG production. Our results suggest that RGD can act as a mechanoreceptor to inhibit collagen production (at low RGD concentrations), but stimulate GAG synthesis (at higher RGD concentrations).

CONCLUSIONS

We demonstrate the ability to regulate biomechanical cues through manipulations in the gel structure, which influences the level of cell deformation, and the gel chemistry to introduce cell–matrix interactions, which serve as mechanoreceptors. The type of loading regime greatly influences the anabolic and catabolic activities of chondrocytes, and therefore may significantly affect the overall quality of the engineered tissue. Together, our long-term research goals are to exploit the gel architecture and chemistry to develop tissue engineering strategies that guide functional tissue growth for cartilage repair.

ACKNOWLEDGEMENTS

The authors acknowledge financial support from the NIH with a research grant from the NIDCR (K22 DE016608). The authors also acknowledge support from the Department of Education's Graduate Assistantships in Areas of National Need Fellowship to GDN and IV and a NASA Harriet Jenkins Predoctoral Fellowship to IV.

REFERENCES

1. S. J. Bryant, and K. S. Anseth. Hydrogel properties influence ecm production by chondrocyte photoencapsulated in poly(ethylene glycol) hydrogels. *J. Biomed. Mater. Res*. **59**:63–72 (2002).
2. S. J. Bryant, C. R. Nuttelman, and K. S. Anseth. Cytocompatibility of ultraviolet and visible light photoinitiating systems on cultured nih/3t3 fibroblasts *in vitro*. *J. Biomater. Sci. Polym. Ed*. **11**:439–457 (2000).
3. J. Elisseeff, K. Anseth, D. Sims, W. McIntosh, M. Randolph, and R. Langer. Transdermal photopolymerization for minimally invasive implantation. *Proc. Natl. Acad. Sci. U. S. A*. **96**:3104–3107 (1999).
4. J. A. Burdick, M. N. Mason, A. D. Hinman, K. Thorne, and K. S. Anseth. Delivery of osteoinductive growth factors from degradable peg hydrogels influences osteoblast differentiation and mineralization. *J. Control. Release*. **83**:53–63 (2002).
5. A. S. Sawhney, C. P. Pathak, and J. A. Hubbell. Bioerodible hydrogels based on photopolymerized poly(ethylene glycol)-co-poly(alpha-hydroxy acid) diacrylate macromers. *Macromolecules*. **26**:581–587 (1993).
6. A. T. Metters, K. S. Anseth, and C. N. Bowman. Fundamental studies of a novel, biodegradable peg-b-pla hydrogel. *Polymer*. **41**:3993–4004 (2000).
7. K. A. Smeds, and M. W. Grinstaff. Photocrosslinkable polysaccharides for *in situ* hydrogel formation. *J. Biomed. Mater. Res*. **54**:115–121 (2001).
8. P. Martens, and K. S. Anseth. Characterization of hydrogels formed from acrylate modified poly(vinyl alcohol) macromers. *Polymer*. **41**:7715–7722 (2000).
9. J. Baier Leach, K. A. Bivens, C. W. Patrick, and C. E. Schmidt. Photocrosslinked hyaluronic acid hydrogels: Natural, biodegradable tissue engineering scaffolds. *Biotechnol. Bioeng*. **82**:578–589 (2003).
10. S. J. Bryant, K. A. Davis-Areharet, N. Luo, R. K. Shoemaker, J. A. Arthur, and K. S. Anseth. Synthesis and characterization of photopolymerized multifunctional hydrogels: Water-soluble poly (vinyl alcohol) and chondroitin sulfate macromers for chondrocyte encapsulation. *Macromolecules*. **37**:6726–6733 (2004).
11. D. A. Wang, C. G. Williams, Q. A. Li, B. Sharma, and J. H. Elisseeff. Synthesis and characterization of a novel degradable phosphate-containing hydrogel. *Biomaterials*. **24**:3969–3980 (2003).
12. Q. Li, C. G. Williams, D. D. N. Sun, J. Wang, K. Leong, and J. H. Elisseeff. Photocrosslinkable polysaccharides based on chondroitin sulfate. *J. Biomed. Mater. Res. A*. **68A**:28–33 (2004).
13. Y. Yeo, J. A. Burdick, C. B. Highley, R. Marini, R. Langer, and D. S. Kohane. Peritoneal application of chitosan and uv-crosslinkable chitosan. *J. Biomed. Mater. Res. A*. **78A**:668–675 (2006).
14. S. H. M. Sontjens, D. L. Nettles, M. A. Carnahan, L. A. Setton, and M. W. Grinstaff. Biodendrimer-based hydrogel scaffolds for cartilage tissue repair. *Biomacromolecules*. **7**:310–316 (2006).
15. J. Elisseeff, W. McIntosh, K. Anseth, S. Riley, P. Ragan, and R. Langer. Photoencapsulation of chondrocytes in poly(ethylene oxide)-based semi-interpenetrating networks. *J. Biomed. Mater. Res*. **51**:164–171 (2000).
16. N. S. Hwang, S. Varghese, Z. Zhang, and J. Elisseeff. Chondrogenic differentiation of human embryonic stem cell-derived cells in arginine-glycine-aspartate modified hydrogels. *Tissue Eng*. **12**:2695–2706 (2006).
17. S. J. Bryant, K. L. Durand, and K. S. Anseth. Manipulations in hydrogel chemistry control photoencapsulated chondrocyte behavior and their extracellular matrix production. *J. Biomed. Mater. Res. A*. **67A**:1430–1436 (2003).
18. M. Dadsetan, J. P. Szatkowski, M. J. Yaszemski, and L. C. Lu. Characterization of photo-cross-linked oligo[poly(ethylene glycol) fumarate] hydrogels for cartilage tissue engineering. *Biomacromolecules*. **8**:1702–1709 (2007).
19. J. A. Burdick, and K. S. Anseth. Photoencapsulation of osteoblasts in injectable rgd-modified peg hydrogels for bone tissue engineering. *Biomaterials*. **23**:4315–4323 (2002).
20. D. S. W. Benoit, A. R. Durney, and K. S. Anseth. Manipulations in hydrogel degradation behavior enhance osteoblast function and mineralized tissue formation. *Tissue Eng*. **12**:1663–1673 (2006).
21. D. A. Wang, C. G. Williams, F. Yang, N. Cher, H. Lee, and J. H. Elisseeff. Bioresponsive phosphoester hydrogels for bone tissue engineering. *Tissue Eng*. **11**:201–213 (2005).
22. M. J. Mahoney, and K. S. Anseth. Three-dimensional growth and function of neural tissue in degradable polyethylene glycol hydrogels. *Biomaterials*. **27**:2265–2274 (2006).
23. V. A. Liu, and S. N. Bhatia. Three-dimensional photopatterning of hydrogels containing living cells. *Biomed. Microdevices*. **4**:257–266 (2002).
24. S. Gerecht, J. A. Burdick, L. S. Ferreira, S. A. Townsend, R. Langer, and G. Vunjak-Novakovic. Hyaluronic acid hydrogen for controlled self-renewal and differentiation of human embryonic stem cells. *Proc. Natl. Acad. Sci. U. S. A*. **104**:11298–11303 (2007).
25. G. M. Cruise, D. S. Scharp, and J. A. Hubbell. Characterization of permeability and network structure of interfacially photopolymerized poly(ethylene glycol) diacrylate hydrogels. *Biomaterials*. **19**:1287–94 (1998).

26. N. A. Peppas, J. Z. Hilt, A. Khademhosseini, and R. Langer. Hydrogels in biology and medicine: From molecular principles to bionanotechnology. *Adv. Mater.* **18**:1345–1360 (2006).
27. M. N. Mason, A. T. Metters, C. N. Bowman, and K. S. Anseth. Predicting controlled-release behavior of degradable pla-b-peg-b-pla hydrogels. *Macromolecules*. **34**:4630–4635 (2001).
28. M. M. Knight, D. A. Lee, and D. L. Bader. Distribution of chondrocyte deformation in compressed agarose gel using confocal microscopy. *Cell. Eng*. **1**:97–102 (1996).
29. P. M. Freeman, R. N. Natarajan, J. H. Kimura, and T. P. Andriacchi. Chondrocyte cells respond mechanically to compressive loads. *J. Orthop. Res*. **12**:311–320 (1994).
30. I. Villanueva, D. S. Hauschulz, D. Mejic, and S. J. Bryant. Static and dynamic compressive strains influence nitric oxide production and chondrocyte bioactivity when encapsulated in peg hydrogels of different crosslinking densities. *Osteoarthr. Cartil.* in press (2008).
31. G. D. Nicodemus, I. Villanueva, and S. J. Bryant. Mechanical stimulation of tmj condylar chondrocytes encapsulated in peg hydrogels. *J. Biomed. Mater. Res. A*. **83A**:323–331 (2007).
32. P. Chomczynski. A reagent for the single-step simultaneous isolation of rna, dna and proteins from cell and tissue samples. *Biotechniques*. **15**:532–& (1993).
33. L. Galois, S. Hutasse, D. Cortial, C. F. Rousseau, L. Grossin, M. C. Ronziere, D. Herbage, and A. M. Freyria. Bovine chondrocyte behaviour in three-dimensional type i collagen gel in terms of gel contraction, proliferation and gene expression. *Biomaterials*. **27**:79–90 (2006).
34. A. P. Hollander, T. F. Heathfield, C. Webber, Y. Iwata, R. Bourne, C. Rorabeck, and A. P. Poole. Increased damage to type-ii collagen in osteoarthritic articular-cartilage detected by a new immunoassay. *J. Clin. Invest*. **93**:1722–1732 (1994).
35. R. W. Farndale, D. J. Buttle, and A. J. Barrett. Improved quantitation and discrimination of sulfated glycosaminoglycans by use of dimethylmethylene blue. *Biochim. Biophys. Acta*. **883**:173–177 (1986).
36. Y. J. Kim, R. L. Y. Sah, J. Y. H. Doong, and A. J. Grodzinsky. Fluorometric assay of DNA in cartilage explants using hoechst-33258. *Anal. Biochem*. **174**:168–176 (1988).
37. F. Guilak, W. R. Jones, H. P. Ting-Beall, and G. M. Lee. The deformation behavior and mechanical properties of chondrocytes in articular cartilage. *Osteoarthr. Cartil*. **7**:59–70 (1999).
38. M. M. Knight, J. M. Ross, A. F. Sherwin, D. A. Lee, D. L. Bader, and C. A. Poole. Chondrocyte deformation within mechanically and enzymatically extracted chondrons compressed in agarose. *Biochim. Biophys. Acta*. **1526**:141–146 (2001).
39. F. Guilak, L. G. Alexopoulos, M. L. Upton, I. Youn, J. B. Choi, L. Cao, L. A. Setton, and M. A. Haider. The pericellular matrix as a transducer of biomechanical and biochemical signals in articular cartilage. *Ann. N. Y. Acad. Sci*. **1068**:498–512 (2006).
40. R. L. Mauck, M. A. Soltz, C. C. B. Wang, D. D. Wong, P. H. G. Chao, W. B. Valhmu, C. T. Hung, and G. A. Ateshian. Functional tissue engineering of articular cartilage through dynamic loading of chondrocyte-seeded agarose gels. *J. Biomech. Eng*. **122**:252–260 (2000).
41. R. L. Mauck, B. A. Byers, X. Yuan, and R. S. Tuan. Regulation of cartilaginous ecm gene transcription by chondrocytes and mscs in 3d culture in response to dynamic loading. *Biomech. Model. Mechanobiol.* **6**:113–125 (2007).
42. J. B. Fitzgerald, M. Jin, D. Dean, D. J. Wood, M. H. Zheng, and A. J. Grodzinsky. Mechanical compression of cartilage explants induces multiple time-dependent gene expression patterns and involves intracellular calcium and cyclic amp. *J. Biol. Chem*. **279**:19502–19511 (2004).
43. J. N. A. De Croos, S. S. Dhaliwal, M. D. Grynpas, R. M. Pilliar, and R. A. Kandel. Cyclic compressive mechanical stimulation induces sequential catabolic and anabolic gene changes in chondrocytes resulting in increased extracellular matrix accumulation. *Matrix Biology*. **25**:323–331 (2006).
44. G. Sharma, R. K. Saxena, and P. Mishra. Differential effects of cyclic and static pressure on biochemical and morphological properties of chondrocytes from articular cartilage. *Clin. Biomech*. **22**:248–255 (2007).
45. C. A. Poole. Articular cartilage chondrons: Form, function and failure. *J. Anat*. **191**:1–13 (1997).
46. E. Ruoslahti. Rgd and other recognition sequences for integrins. *Annu. Rev. Cell Dev. Biol*. **12**:697–715 (1996).
47. M. Enomoto-Iwamoto, M. Iwamoto, K. Nakashima, Y. Mukudai, D. Boettiger, M. Pacifici, K. Kurisu, and F. Suzuki. Involvement of alpha 5 beta 1 integrin in matrix interactions and proliferation of chondrocytes. *J. Bone Miner. Res*. **12**:1124–1132 (1997).
48. C. N. Salinas, B. B. Cole, A. M. Kasko, and K. S. Anseth. Chondrogenic differentiation potential of human mesenchymal stem cells photoencapsulated within poly(ethylene glycol)-arginine-glycine-aspartic acid-serine thiol-methacrylate mixed-mode networks. *Tissue Eng*. **13**:1025–1034 (2007).